ELSEVIER

Contents lists available at ScienceDirect

Remote Sensing of Environment

journal homepage: www.elsevier.com/locate/rse



Disturbance detection in landsat time series is influenced by tree mortality agent and severity, not by prior disturbance



Kyle C. Rodman^{a,*}, Robert A. Andrus^b, Thomas T. Veblen^c, Sarah J. Hart^a

- ^a Department of Forest and Wildlife Ecology, University of Wisconsin, Madison, WI, United States
- ^b School of the Environment, Washington State University, Pullman, WA, United States
- ^c Department of Geography, University of Colorado, Boulder, CO, United States

ARTICLE INFO

Keywords:
Bark beetle
Event detection
Ground truth
LandTrendr
Multiple disturbances
Overlapping disturbances
Spruce beetle
Wildfire

ABSTRACT

Landsat time series (LTS) and associated change detection algorithms are useful for monitoring the effects of global change on Earth's ecosystems, Because LTS algorithms can be easily applied across broad areas, they are commonly used to map changes in forest structure due to wildfire, insect attack, and other important drivers of tree mortality. But factors such as initial forest density, tree mortality agent, and disturbance severity (i.e., percent tree mortality) influence patterns of surface reflectance and may influence the accuracy of LTS algorithms. And while LTS algorithms are widely used in areas with a history of multiple disturbance events during the Landsat record, the effectiveness of LTS algorithms in these conditions is not well understood. We compared products from the LTS algorithm LandTrendr (Landsat-based Detection of Trends in Disturbance and Recovery) with a unique field dataset from a landscape heavily influenced by both wildfire and spruce beetles (Dendroctonus rufipennis) since c. 2000. We also compared LandTrendr to other common methods of mapping fire- and spruce beetle-affected areas. We found that LandTrendr more accurately detected wildfire than spruce beetle-induced tree mortality, and both mortality agents were more easily detected when they occurred at high severity. Surprisingly, prior spruce beetle outbreaks did not influence the detectability of subsequent wildfire. Compared to alternative disturbance mapping approaches, LandTrendr predicted a c. 40% lower area affected by wildfire or spruce beetle outbreaks. Our findings indicate that disturbance type- and severity-specific differences in omission error may have broad implications for disturbance mapping efforts that utilize Landsat data. Gradual, lowseverity disturbances (e.g., background tree mortality and non-stand replacing disturbance) are pervasive in forest ecosystems, yet they can be difficult to detect using automated LTS algorithms. Whenever possible, methods to account for these biases should be incorporated in LTS-based mapping efforts, including the use of multispectral ensembles and ancillary spatial data to refine predictions. However, our findings also indicate that LTS algorithms appear to be robust in areas with multiple disturbance events, which is important because these areas will increase as new acquisitions extend the length of the Landsat record.

1. Introduction

Climate change is altering patterns of ecological disturbance across Earth's forested ecosystems (McDowell et al., 2020; Turner, 2010). As relatively discrete events that reduce plant biomass (Grime, 1979), disturbances can have lasting influences on forest structure, with cascading effects on carbon storage and other important ecosystem services (Bonan, 2008; Thom and Seidl, 2016). Remotely sensed data play a key role in monitoring forest disturbances because they provide a consistent record across expansive areas (Trumbore et al., 2015). In particular, imagery from the Landsat program has been widely used in

studies of forest ecosystems because these data have a relatively high spatial resolution (c. 30–60 m) and an unmatched temporal extent (c. 50 years) (Wulder et al., 2019). To leverage this extended data record, several algorithms have been recently developed to detect changes in surface cover using Landsat image time series (LTS) (e.g., Hermosilla et al., 2016; Huang et al., 2010; Hughes et al., 2017; Kennedy et al., 2010; Zhu et al., 2020). Common goals for LTS algorithms are to 1) separate distinct change events (i.e., signal) from inter- or sub-annual spectral variation (i.e., noise) with little direct input from the analyst and 2) characterize the timing, duration, and spectral magnitude of events (Banskota et al., 2014; Zhu, 2017). By quantifying the timing and

E-mail address: krodman2@wisc.edu (K.C. Rodman).

^{*} Corresponding author.

magnitude of spectral changes, LTS methods can improve the representation of ecological processes such as disturbance and recovery (Kennedy et al., 2014).

Though LTS algorithms offer a promising approach for forest ecosystem monitoring, validation is critical for characterizing patterns of change and making inferences about ecological processes (Pengra et al., 2016; Thomas et al., 2011). The most common validation approaches for LTS algorithms include comparisons with simulated data (Awty-Carroll et al., 2019) and analyst interpretations of LTS trajectories alongside high-resolution imagery (Cohen et al., 2017). When available, field data are highly valuable, particularly in identifying agents of tree mortality, quantifying disturbance severity (i.e., percent tree mortality), and characterizing subcanopy effects that are not always apparent in imagery (Schroeder et al., 2014). However, comparisons with field data are uncommon because data collection costs are high and field surveys rarely capture consistent information before and after individual disturbance events (Cohen et al., 2010; Thomas et al., 2011). Field data provide an important and underutilized supplement to other reference data by connecting spectral trajectories in LTS with the ecological

processes that are occurring throughout forested ecosystems.

Forest structure and the characteristics of individual disturbance events influence the spectral signal associated with tree mortality and have the potential to affect LTS detection (Fig. 1a). For instance, observed spectral change increases with disturbance severity and initial forest density (Harvey et al., 2019; Meigs et al., 2015; Miller et al., 2009); low levels of tree mortality typically cause minimal spectral change that is difficult to distinguish from interannual variability and may go undetected by LTS algorithms (Cohen et al., 2010). Additionally, different disturbance types have unique spectral characteristics and varying durations at the scale of a Landsat cell (Fig. 1a). Tree mortality caused by rapid and temporally-discrete disturbances (e.g., wildfire or timber harvest) may be more easily detected than mortality caused by disturbances that unfold over several years or more (e.g., tree-killing insects) (Schleeweis et al., 2020). Furthermore, when multiple disturbance events occur in the same location within the Landsat record (i.e., the 1970s to present), their interaction has the potential to influence LTS detection. For instance, initial forest disturbances may alter the spectral characteristics of subsequent disturbances (Harvey et al., 2019; Parks

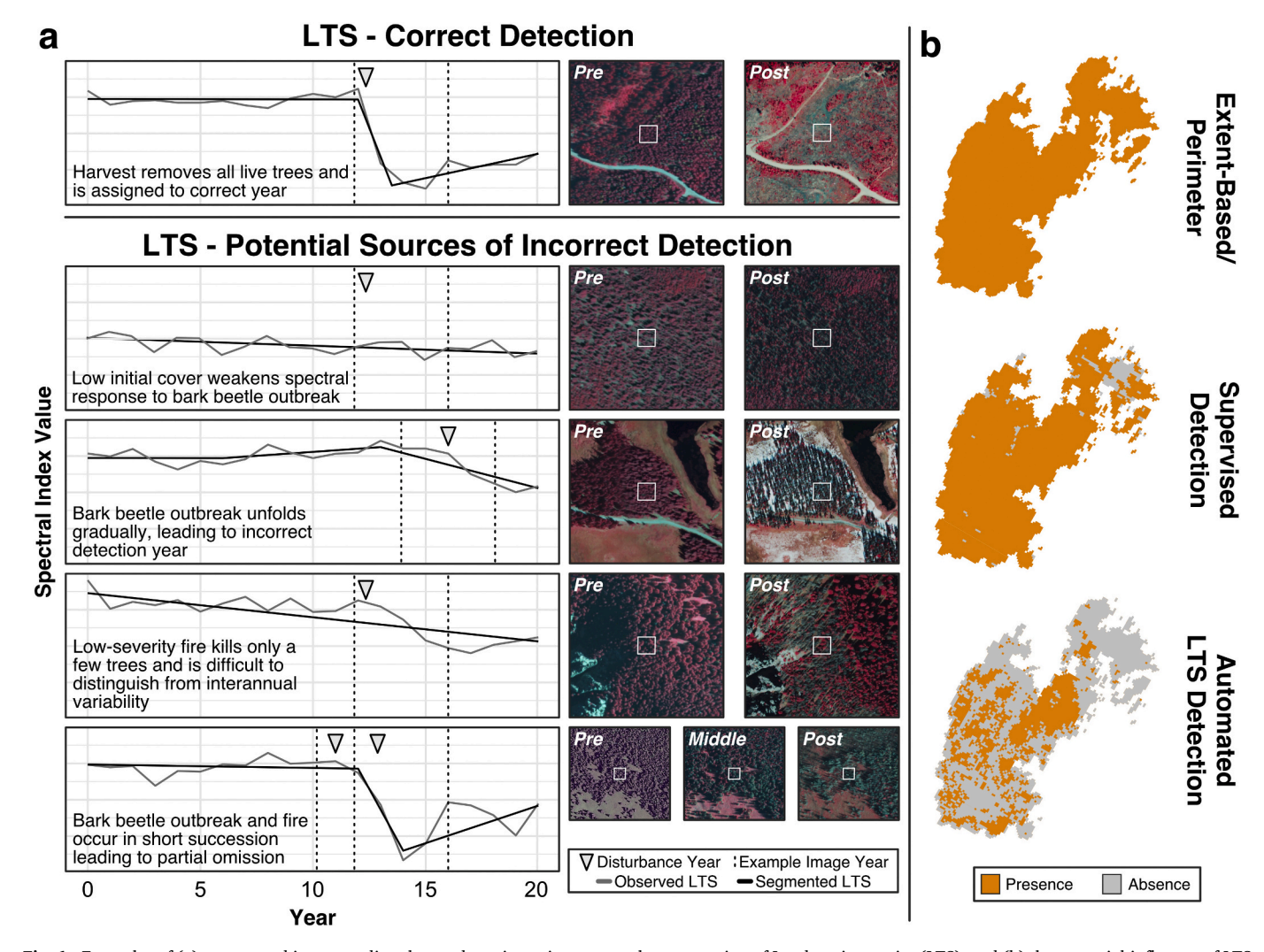


Fig. 1. Examples of (a) correct and incorrect disturbance detection using temporal segmentation of Landsat time series (LTS), and (b) the potential influence of LTS detection error on broad-scale disturbance mapping. In (a), line graphs give observed (grey) and segmented (black) spectral values from example LTS trajectories in subalpine forests throughout southwestern Colorado, USA. The true year of disturbance occurrence is indicated by triangles above LTS trajectories, and the timing of pre/post image acquisition is indicated by dashed lines. Image panels are false-colour composites (red highlights live vegetation) of 1-m aerial photography from the National Agriculture Imagery Program (NAIP; USFS NAIP, 2020) collected before and after individual disturbances; white boxes in NAIP images correspond to the location of each LTS trajectory. We expected that (a) sources of detection error in LTS algorithms would lead to lower estimates of disturbed area when compared to (b) alternative approaches such as mapped perimeters of the total affected area (e.g., fire perimeters) or analyst-supervised detection methods such as image classification or two-date change indices. (For interpretation of the references to colour in this figure legend, the reader is referred to the web version of this article.)

et al., 2014) and thereby influence detectability in LTS. Similarly, when two or more disturbance events occur in short succession, the spectral trajectory may appear similar to a single disturbance spanning several years (Fig. 1a), masking potentially meaningful differences in disturbance effects (e.g., compound effects; Paine et al., 1998). Though LTS methods are widely applied in areas with overlapping disturbances (e.g., Hermosilla et al., 2019; Schleeweis et al., 2020; White et al., 2017), the ability of LTS algorithms to detect these events is poorly understood.

In forests of the western United States, wildfire and bark beetle (Curculionidae: Scolytinae) outbreaks are two of the most important drivers of tree mortality, where they have affected at least 6.3% and 7.1% of the total forested area over the past three decades (Hicke et al., 2016). Because fire and bark beetle outbreaks can have major influences on forest ecosystems, LTS detection and other mapping methods are commonly used to quantify disturbance-affected areas at a range of spatial scales (e.g., Meigs et al., 2015; Schroeder et al., 2011; Senf et al., 2015). Previously mapped fire perimeters (e.g., Canadian National Fire Database, Monitoring Trends in Burn Severity) or aerial sketches of insect-affected area (e.g., Aerial Detection Surveys, Aerial Overview Surveys) can help to characterize disturbance extent at national or regional levels (e.g., Bentz et al., 2009; Hanes et al., 2019). Though this extent-based approach permits rapid calculations across broad areas, mapped perimeters typically include areas without tree mortality, leading to notable overestimates of the affected area (Kolden et al., 2012; Meddens et al., 2016). Alternatively, approaches such as image classification (e.g., Hart and Veblen, 2015; Meddens et al., 2013; Schroeder et al., 2014) or two-date change indices (e.g., Meddens et al., 2016; Meigs et al., 2020) can be used to map finer-grain estimates of tree mortality, but these approaches require more direct input from analysts and thus a greater investment of time. Different mapping methods including LTS detection, extent-based approaches, and analystsupervised detection - may give substantial differences in estimates of disturbance-affected area (Fig. 1b).

Using a unique field dataset describing forest structure, causes of tree mortality, and disturbance severity in a landscape affected by bark beetle outbreaks and wildfire since c. 2000, we evaluated the ability of the LTS algorithm LandTrendr (Landsat-based Detection of Trends in Disturbance and Recovery; Kennedy et al., 2010) to identify the occurrence and timing of individual disturbance events. Given our focus on disturbance detection, we used LandTrendr, one of the most widely applied LTS algorithms (Zhu, 2017) because it has lower rates of omission than many comparable tools (Cohen et al., 2017). To determine the extent to which LTS disturbance detection matched other estimates of disturbed area, we also compared LandTrendr products with additional mapping methods (i.e., fire perimeters, aerial surveys of insect-induced tree mortality, two-date change indices of fire severity, and a supervised classification of insect-affected area) available in the study area. Specifically, we asked the following questions:

Q1. How do pre-disturbance forest density, mortality agent, disturbance severity, and time between overlapping disturbances influence detectability in LTS? We expected that overlapping disturbances would be easiest to detect in LTS when they occurred in areas with dense forest cover, were temporally abrupt, occurred at high severity, and were separated by longer intervals.

Q2. How do estimates of disturbance occurrence and overlap differ among common methods of detection? We expected that extent-based approaches using wildfire perimeters and aerial surveys of bark beetle outbreaks would give the largest estimates of disturbance-affected area, and LTS products would give the smallest estimates because of partial omission.

2. Methods

2.1. 2.1. Study area and focal disturbance types

Our study area is within the boundaries of five wildfires that

occurred in 2012 and 2013 throughout the San Juan Mountains in southwestern Colorado, U.S.A. (Table 1, Fig. 2). Forests in the San Juan Mountains span a broad elevational range (c. 1500–3600 m); subalpine forests (2700–3600 m) comprise the core of the mountain range (Romme et al., 2009) and make up 87% of the total area within the studied fires (Rollins, 2009). The dominant tree species in subalpine forests of the San Juan Mountains include Engelmann spruce (*Picea engelmannii*), subalpine fir (*Abies lasiocarpa*), and quaking aspen (*Populus tremuloides*) (Wilson et al., 2013). Climate varies dramatically across elevational gradients in the study area. Average annual precipitation ranges from 400 to 1600 mm year $^{-1}$, January minimum temperatures range - 20 to -11 °C, and July maximum temperatures range 17 to 28 °C (1981–2010 normals; PRISM, 2020).

Wildfire and bark beetles (e.g., Dendroctonus spp., Ips spp., Dryocoetes spp.) have long shaped the structure of subalpine forests in the southern Rocky Mountains, U.S.A. (Baker and Veblen, 1990). Fires are typically infrequent and stand-replacing in subalpine forests, constrained to exceptionally dry conditions that are suitable for widespread burning (Buechling and Baker, 2004; Sibold and Veblen, 2006), such as the weather conditions that occurred during the 2012-2013 fires studied here (Andrus et al., 2016). Spruce beetle (Dendroctonus rufipennis) is the most important tree-killing insect in subalpine forests of the San Juan Mountains, where it primarily attacks Engelmann spruce and occasionally blue spruce (Picea pungens). Stands composed of abundant large-diameter spruce are most susceptible to spruce beetle attack (Jenkins et al., 2014; Schmid and Frye, 1977; Temperli et al., 2014), and warm, dry periods can initiate epidemic-level outbreaks across broad areas (Hart et al., 2014; Raffa et al., 2008). Western balsam bark beetle (WBBB; Dryocoetes confusus) is another notable tree-killing insect in subalpine forests of the San Juan Mountains, where it primarily affects subalpine fir; though widespread, WBBB outbreaks typically occur at lower severity than do spruce beetle outbreaks (Andrus et al., 2020; Lalande et al., 2020) and were not a focus of this study. Recently, the combined effects of spruce beetle and fire have led to notable changes in forest structure throughout the San Juan Mountains (Andrus et al., 2020; Carlson et al., 2017; Savage et al., 2017). In our study area, a spruce beetle outbreak began in the early 2000s (Hart et al., 2017) and the stand-scale effects of the outbreak ranged from minor mortality to neartotal mortality of mature trees (Table 1). Similarly, the 2012 and 2013 fires had a range of effects on stand structure, though severity was generally high (Table 1).

Table 1Fire name, number of field plots, year of fire occurrence, fire severity, years of the initial detection of spruce beetle-induced tree mortality, and pre-fire spruce beetle severity in each of the five surveyed sites in southwestern Colorado, USA. Fire severity, years of spruce beetle detection, and spruce beetle severity are summarized for field plots, not at the extent of each site.

Fire Name	No. Field Plots	Fire Year	Fire Size (ha)	Fire Severity ^c	Years of Spruce Beetle Detection ^d	Spruce Beetle Severity ^c
East Fork	2	2013	142	58 (16–100)	2005–2008	52 (28–77)
Little Sand	11	2012	10,089	66 (29–100)	2000–2009	23 (7–91)
Papoose	39	2013	19,978	95 (3–100)	2000–2010	73 (9–96)
West Fork	50	2013	22,895	95 (0-100)	2000–2010	79 (34–99)
Windy Pass	11	2013	574	89 (11–100)	2001–2010	68 (22–95)

^c Fire severity and spruce beetle severity are the median (min-max) percentage of pre-disturbance live tree basal area killed in field plots

^d Years of spruce beetle activity were determined for each field plot based on analyst interpretation of Landsat time series from 1984 to 2019, US Forest Service Aerial Detection Survey data from 1996 to 2019, and high resolution (1-m) aerial photography collected in 2005, 2009, 2011, 2013, 2015, and 2017

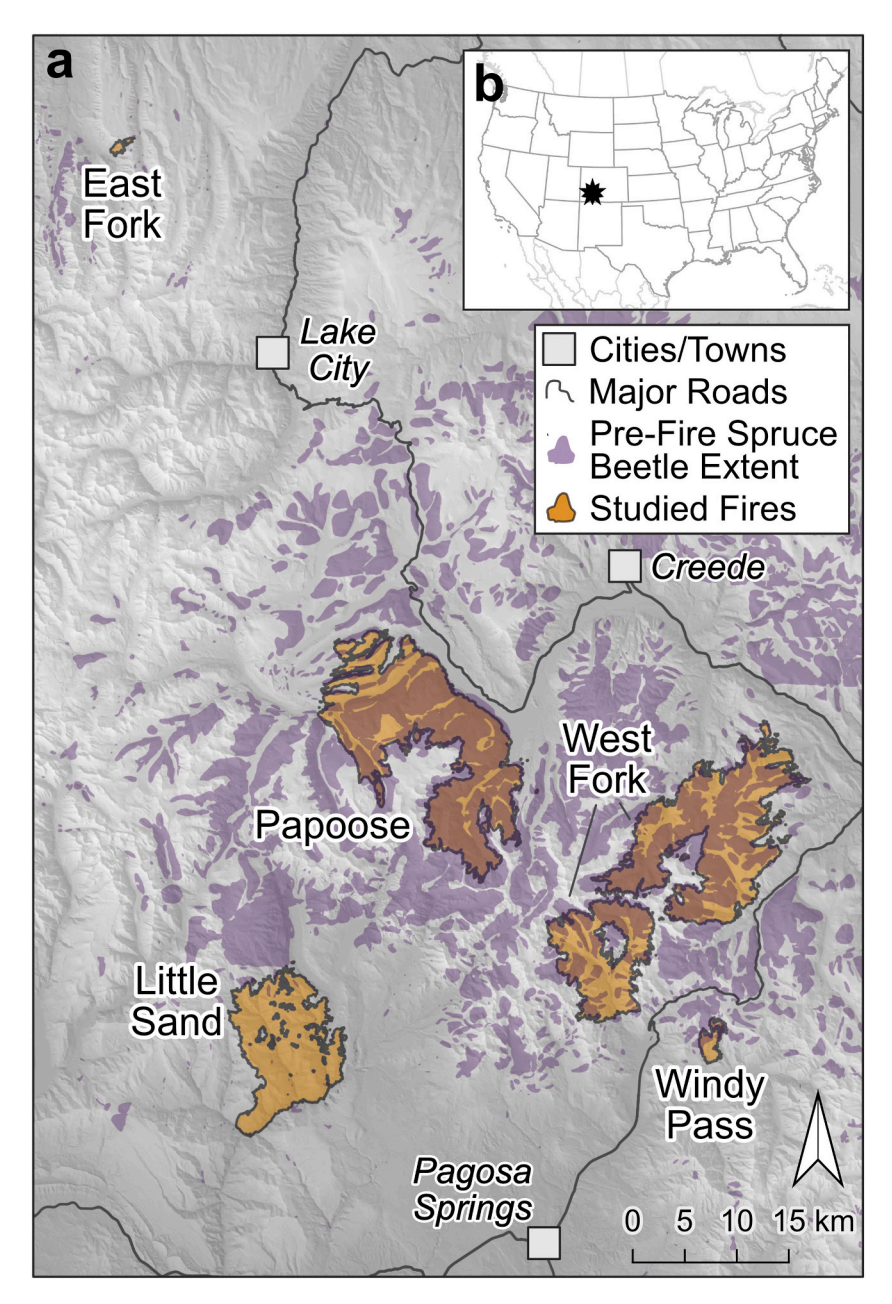


Fig. 2. Site map showing the locations of the five studied fires in southwestern Colorado, USA. Pre-fire spruce beetle (*Dendroctonus rufipennis*) extent is based on US Forest Service Aerial Detection Surveys (USFS ADS, 2020) of tree mortality 1996–2012 (i.e., before all fires except for the 2012 Little Sand). Each fire was surveyed in the field for tree mortality due to spruce beetle and wildfire (Andrus et al., 2016).

2.2. Datasets

2.2.1. Development of Landsat time series

We used Google Earth Engine (GEE; Gorelick et al., 2017) to extract and process all Landsat Tier 1 Surface Reflectance scenes (geometrically and atmospherically corrected) from 1984 to 2019 that overlapped the study area and were collected during the growing season of the subalpine zone (i.e., July 1–September 30). These data included imagery from the Landsat 5 Thematic Mapper (TM), Landsat 7 Enhanced Thematic Mapper Plus (ETM+), and Landsat 8 Operation Land Imager (OLI). Because of reflective wavelength differences between TM/ETM+ and OLI sensors, we harmonized Landsat 8 OLI bands to TM/ETM+ equivalents following Roy et al. (2016). Within each scene, we masked pixels obstructed by clouds, shadows, and snow using the CFMask-derived quality assurance band (Foga et al., 2017). We created annual composite images from the individual scenes using medoid selection (Flood,

2013). Because LandTrendr operates on a single band or spectral index, we used annual composite images to develop 1984–2019 time series of the Normalized Burn Ratio (NBR) (Key and Benson, 2006). NBR, the normalized difference between TM-equivalent bands four (0.76–0.90 μm) and seven (2.09–2.35 μm), has been widely used in prior studies of fire and tree-killing insects (Meigs et al., 2015; Senf et al., 2017, 2015).

2.2.2. LTS disturbance detection

To test the ability of LTS methods to identify tree mortality due to wildfire and spruce beetle outbreaks throughout the study area, we used the GEE implementation of LandTrendr (Kennedy et al., 2018). LandTrendr is a pixel-based algorithm that uses temporal segmentation of LTS to identify important features (i.e., segments; homogenous periods of change or stability) while excluding noise due to atmospheric and geometric distortion, interannual climate variability, vegetation phenology, and changes in illumination (Kennedy et al., 2010). For

segmentation parameters in LandTrendr (e.g., spike threshold, p-value threshold, the maximum number of segments), we used values in Table 1 of Kennedy et al. (2018). Rather than optimizing parameters for the study area, our goal was to compare LandTrendr products developed using standard practices with reference data. A sensitivity analysis of the effect of parameter values on segmentation accuracy confirmed that results were relatively insensitive to parameter selection (Appendix A). A minimum mapping unit (MMU) filter by detection year is sometimes used as a noise-reduction technique to account for the spatial context surrounding each voxel (e.g., Kennedy et al., 2012). We did not use an MMU filter because insect outbreaks can spread gradually through a stand, leading to slight differences in the timing of detection in adjacent 30-m pixels. For comparison with field data and alternative methods of mapping disturbance, we extracted the year of detection as well as the direction and magnitude of spectral change from each LandTrendrderived segment in each 30-m cell.

2.2.3. Field data

We compared LandTrendr products with previously collected field data from 141 plots (20 × 20 m) in Engelmann spruce- and subalpine firdominated forests throughout the study area (Fig. 2, Table 1) (Andrus et al., 2016). These data, collected using established methods (Harvey et al., 2013), are field surveys of pre-fire tree mortality due to spruce beetle (e.g., reconstructed primarily from tree attributes and cambial evidence of spruce beetle attack) as well as fire effects (e.g., tree mortality, percent surface charring). For analyses, we used a subset of 113 plots that 1) had at least some (i.e., greater than zero) pre-fire tree mortality due to spruce beetle, 2) had wildfire activity observed on the plot, either through tree mortality or surface charring, and 3) had three or more years between the onset of tree mortality due to spruce beetle and wildfire occurrence. Three or more years between outbreak onset and wildfire occurrence allowed for non-overlapping one-year buffers surrounding the year of each disturbance to account for uncertainty in the detection year (discussed further in 2.3.1. Statistical Comparisons of Field Data and LTS Detection). Using these data, we calculated pre-spruce beetle (c. 2000) and pre-fire (c. 2012) live basal area for all trees exceeding 4 cm in diameter at breast height (DBH, 1.37 m above ground level). We then calculated plot-level spruce beetle severity and fire severity as the percentage of pre-outbreak basal area killed by spruce beetle, and the percentage of live pre-fire basal area killed by fire, respectively. The severity of each disturbance type ranged widely (7–99% for spruce beetle and 0–100% for fire; Table 1) and these metrics were not correlated at the plot-level (Pearson's r < 0.01).

2.2.4. Identifying the timing of spruce beetle outbreak in field plots

Bark beetle outbreaks have a typical duration of c. 3-4 years at the 30-m scale of a Landsat cell (Meddens and Hicke, 2014), and the timing of disturbance is not easily defined without repeated field surveys or detailed interpretation of multi-temporal data. Herein, a single analyst assigned a year of spruce beetle "outbreak detection" to each field plot, in which the onset of tree mortality could be visually identified based on the following reference datasets: 1) 1-m imagery from the National Agriculture Imagery Program (NAIP; USFS NAIP, 2020) collected in 2005, 2009, 2011, 2013, 2015, and 2017, 2) US Forest Service Aerial Detection Surveys (ADS; USFS ADS, 2020) conducted each year for the period 1996-2019, and 3) 1984-2019 trajectories of NBR and Landsat TM-equivalent band 7 (sensitive to outbreak initiation; Foster et al., 2017). To account for uncertainty in the timing of outbreak detection and disagreement among the reference datasets, the analyst also assigned a confidence rating of high (\pm 0 years), medium (\pm 2 years), or low (\pm 4 years) for each detection year estimate. We included this confidence rating in later statistical models because the confidence of the interpreter in assigning a detection year is related to the quality of the reference data and thus the ability of LandTrendr to match the reference. We note that our definition of outbreak detection refers to the onset of visible tree mortality rather than the timing of initial spruce

beetle infestation, as visible signs of tree mortality often lag infestation (Foster et al., 2017; Meddens and Hicke, 2014). A further description of methods used in determining the timing of spruce beetle outbreak in field plot locations is provided in Appendix B.

2.2.5. Alternative disturbance mapping methods for comparison with LTS detection

To understand how LTS algorithm biases influence the characterization of disturbance-affected area, we also compared LandTrendr disturbance detection to two additional mapping methods that are commonly used for quantifying the area affected by wildfire and bark beetle outbreaks. First, we obtained perimeters for each of the five studied fires from the Wildland Fire Support Geospatial Multi-agency Coordinating Group (GeoMAC, 2020), and ADS-mapped boundaries of spruce beetle affected area between 1996 (the first year in which this portion of the San Juan Mountains was mapped) and 2011 (prior to the occurrence of fires in 2012 and 2013). Using these data, we calculated the area burned as the total area within GeoMAC fire perimeters, and the area of spruce beetle outbreak as the total area of ADS spruce beetle polygons, restricted to areas within fire perimeters. Our second approach, which better identifies undisturbed areas within mapped perimeters (Kolden et al., 2012; Meddens et al., 2016), was to identify burned area using the Relative differenced Normalized Burn Ratio (RdNBR), and spruce beetle presence using a previous NAIP-based classification of grey-stage tree mortality (i.e., greater than c. two years since infestation; Schmid and Frye, 1977). RdNBR is an index of fire severity based on the two-date changes in the Normalized Burn Ratio, relativized by the initial spectral values (Miller and Thode, 2007). The NAIP-based classification of tree mortality attributed to spruce beetle was previously developed at a 3-m spatial resolution using 2011 NAIP imagery with an overall accuracy of c. 90% (Hart and Veblen, 2015).

We calculated RdNBR within each of the studied fires using annual composite images from years preceding and following fire occurrence (following Meigs and Krawchuk, 2018). This approach improves upon standard fire severity products (e.g., Eidenshink et al., 2007) by minimizing the influence of clouds, snow, and shadows in individuals scenes, as well as data gaps caused by the Scan Line Corrector failure in ETM+ (Parks et al., 2018). Because two-date change indices are sensitive to phenological differences between images (Kolden et al., 2015), we applied a phenology offset using unburned forest pixels (identified using the 2016 National Land Cover Dataset; Homer et al., 2020) in a 300-m outward buffer from each fire perimeter. We defined the burned area as all 30-m cells within each fire perimeter with positive RdNBR values, thus excluding unburned cells. To identify areas affected by spruce beetle using the NAIP-based classification, we aggregated these data to a 30-m spatial resolution (aligned with LandTrendr products and RdNBR maps of fire extent). To account for classification uncertainty, we defined spruce beetle presence as all 30-m cells with at least 10% classified cover of grey-stage tree mortality. Because these NAIP-based maps did not overlap with the East Fork fire or the southern portion of the Little Sand fire (8.75% of total fire area), we excluded these areas from all broad-scale spatial analyses. A sensitivity analysis describing the influence of different definitions of disturbance presence on RdNBR- and NAIP-mapped disturbance area is presented in Appendix C.

2.3. Analytical methods

2.3.1. Statistical comparisons of field data and LTS detection

We extracted LandTrendr outputs at the location of each field plot and compared these records to field data describing vegetation structure and disturbance characteristics using two generalized linear mixed models (GLMMs) (Bolker et al., 2009). We developed the first GLMM to examine the influences of initial forest cover, tree mortality agent, disturbance severity, and analyst-interpreted time between events on LandTrendr detection of wildfire and spruce beetle outbreak (hereafter

"two-disturbance model"). We hypothesized that the timing and severity of prior disturbance may have a one-directional influence on the detection of subsequent disturbance. Thus, we developed a second GLMM to quantify the effect of spruce beetle outbreaks on the detection of wildfire (hereafter "fire model"). In each GLMM, the response variable represented correct or incorrect disturbance detection by Land-Trendr. Detection was considered correct if LandTrendr identified the initiation of disturbance within one year of the observed (i.e., fire) or analyst-interpreted (i.e., spruce beetle) detection year. Allowing for a one-year offset helps to account for differences in image collection dates or a lack of clear-sky imagery in portions of annual composites (Cohen et al., 2017, 2010). We used a Bernoulli distribution in each GLMM; we selected a logit link function for the two-disturbance model and a complementary log-log link function for the fire model to account for class imbalance (Zuur et al., 2009). For the two-disturbance model (n =226; two observations in 113 plots), we included a nested random intercept term of plot within fire to account for dependence between observations within a plot and among plots within each fire. For the fire model (n = 113), we included a random intercept term of fire. We developed GLMMs using the 'glmmTMB' package (Brooks et al., 2017) and all statistical analyses were performed in R (R Core Team, 2018) (Appendix D).

We used a model selection approach to identify the most important predictors of LandTrendr disturbance detection. For the two-disturbance model, we included as potential predictors: 1) live basal area of all tree species prior to disturbance occurrence, 2) percent basal area mortality in the disturbance event, 3) the mortality agent (i.e., fire or spruce beetle), 4) the number of years between spruce beetle detection and fire occurrence, and 5) analyst confidence in assigning a specific detection year. For the fire model, we included: 1) live basal area prior to spruce beetle outbreak, 2) live basal area after spruce beetle outbreak but prior to fire, 3) percent of pre-outbreak basal area killed by spruce beetle, 4) percent of pre-fire basal area killed during fire, and 5) the number of years between spruce beetle detection and fire occurrence. Relevant bivariate interaction terms were also included in each set of statistical models (Appendix D). For comparison of effect sizes of categorical (i.e., binary contrasts) and continuous predictors, we scaled all continuous predictors by subtracting the mean and dividing by two standard deviations (Gelman, 2008). For final models, we retained predictors that minimized the sample size-corrected Akaike Information Criterion (AICc) in all possible subsets model selection (the 'dredge' function in the 'MuMIn' package; Bartón, 2018). Following model selection and fitting, we used the 'DHARMa' package (Hartig, 2018) to test residual distributions, and spline correlograms in the 'ncf' package (Bjornstad, 2019) to test for spatial autocorrelation in the residuals. Residuals from final GLMMs met all necessary assumptions (Appendix D).

2.3.2. Comparison of LTS detection with other mapping methods

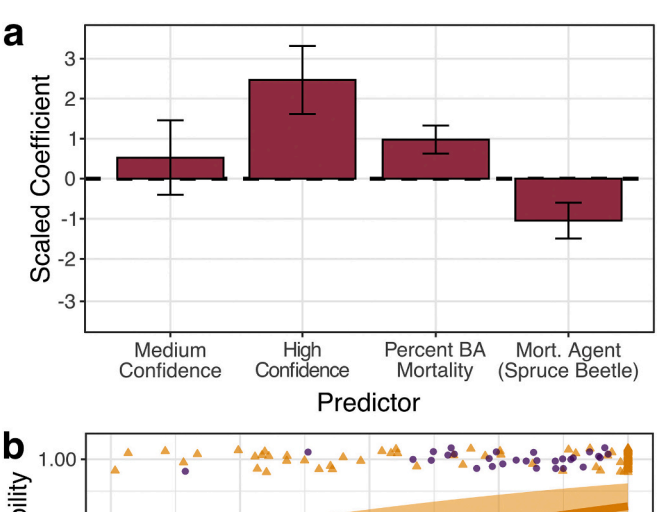
We compared the total mapped area of fire only, spruce beetle outbreak only, fire and spruce beetle overlap, and total undisturbed area using three different mapping methods: 1) GeoMAC and ADS perimeters, 2) RdNBR and NAIP-based maps, and 3) LandTrendr products. For this comparison, we restricted LandTrendr-detected fire events to those within fire perimeters that corresponded to the fire year (2012 for Little Sand and 2013 for the remaining fires). For LandTrendr detection of spruce beetle, we included all disturbance segments initiating 1996-2011. We excluded 2.4% of the total study area where sanitation harvests, salvage logging, and timber harvests were recorded from 1996 to 2011 (USFS Geodata, 2020) from all spruce beetle layers. Similarly, we restricted all maps of spruce beetle activity to forest stands with the presence of Engelmann spruce following Hart and Veblen (2015). Finally, to determine if LandTrendr detection was related to remotely sensed estimates of disturbance severity, we used classification tree models (Breiman et al., 1984) in the 'party' package (Hothorn et al., 2014) in R. Specifically, we compared mapped disturbance severity, represented here using continuous values of RdNBR and NAIP-derived

percent grey-stage tree mortality, in pixels identified as disturbed and undisturbed in LandTrendr maps. For ease of interpretation and to minimize overfitting, we restricted classification trees to a maximum depth of 1 (i.e., a single binary split). We weighted individual observations based on class prevalence to account for imbalanced sampling and assessed final classification accuracy using 10-fold cross-validation.

3. Results

3.1. Comparing LandTrendr disturbance detection to field data

In the two-disturbance GLMM, LandTrendr detection was best predicted by the tree mortality agent (i.e., fire or spruce beetle), percent basal area mortality, and interpreter confidence in the year of disturbance (Fig. 3a; Δ AICc from second-ranked model = 1.7). LandTrendr was less likely to detect spruce beetle outbreak initiation than wildfire ($\beta = -1.02, p = 0.03$; Fig. 3a, b). Specifically, 74.3% of fire disturbances were correctly identified within one year by LandTrendr, compared to just 26.5% for spruce beetle. Though only a portion of spruce beetle disturbances could be assigned with confidence to a specific year (n = 34; 30.1% of the total), the detection rate for these "high-confidence"



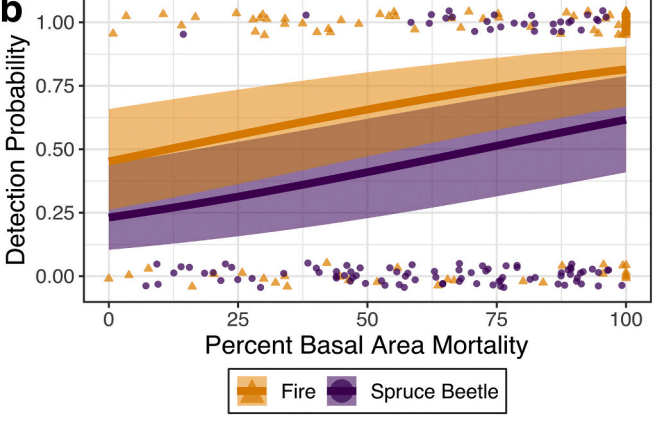


Fig. 3. Results of the final 'two-disturbance' GLMM of LandTrendr detection of wildfire and spruce beetle outbreaks in the San Juan Mountains, CO, USA. (a) Scaled coefficients show the direction and effect size of each predictor included in the final model, and error bars give \pm one standard error of the coefficient estimate. In (a), "Medium Confidence" and "High Confidence" give contrasts with the "Low Confidence" level for the categorical predictor of interpreter confidence when assigning a detection year. In (b), detection probabilities for fire (orange) and spruce beetle (purple) disturbances are given across a range of disturbance severities. Points show the observed data, jittered vertically for clarity. Predicted values (curves with shaded areas representing \pm one standard error of the prediction) are conditional on the mean value of random effects and assume that an interpreter identified a disturbance with high confidence. (For interpretation of the references to colour in this figure legend, the reader is referred to the web version of this article.)

events (i.e., 61.8%) was still 12.5% lower than detection of fire. As expected, interpreter confidence in the year of disturbance was associated with LandTrendr detection (low vs. moderate: $\beta = 0.57$, p = 0.51; low vs. high: $\beta = 2.40$, p < 0.01). Probability of disturbance detection by LandTrendr was positively related to percent basal area mortality (i.e., disturbance severity) for both mortality agents ($\beta = 0.98$, p < 0.01; Fig. 3b). Pre-disturbance live basal area, the time between disturbance events, and bivariate interaction terms were not included in the most parsimonious two-disturbance model. For disturbances that were correctly detected, the spectral magnitude of change in the corresponding disturbance segment was weakly correlated with field-derived percent basal area mortality (Pearson's r=0.25 for spruce beetle; r=0.21 for fire). In the fire model, we found that LandTrendr detection of fire events was primarily related to fire severity ($\beta = 0.71$, p < 0.01; Appendix D), and no other predictors were retained in the top model (Δ AICc from the second-ranked model = 0.71). Contrary to expectations, initial forest cover (i.e., basal area) and the timing and severity of prior spruce beetle disturbance had little influence on the detection of

3.2. Comparing LandTrendr to other mapping methods

When comparing LandTrendr disturbance detection with other methods of quantifying spruce beetle- and fire-affected areas, we found important differences in areal estimates. The mapping approach using GeoMAC fire perimeters and ADS polygons had the greatest area affected by only fire (249.0 km²), as well as the greatest area of overlap between spruce beetle outbreak and fire (281.8 km²) (Fig. 4a, d). RdNBR and NAIP-derived maps of grey-stage tree mortality had the second highest areas affected by only fire (213.5 km²) and spruce beetle and fire overlap (274.3 km²) (Fig. 4b, d). Importantly, this approach also identified unburned areas that were affected by only spruce beetle (13.2 km²) or were unaffected by either disturbance (29.8 km²). Areal estimates derived from thresholding RdNBR and NAIP were relatively insensitive to the threshold used to determine disturbance presence/ absence (Appendix C). In comparison with ADS and GeoMAC perimeters and RdNBR- and NAIP-based maps, LandTrendr estimated a much lower area affected by fire or spruce beetle. Specifically, LandTrendr had lower areas affected by only fire (178.1 km²) and both disturbances (95.9 km²), and a substantially higher undisturbed area (216.8 km²) (Fig. 4b, d). Overall, the LandTrendr estimate of the area affected by fire or bark beetle was 40.8% lower than estimates using ADS and GeoMAC perimeters and 37.3% lower than RdNBR- and NAIP-based maps.

LandTrendr detection was also related to RdNBR fire severity and percent grey-stage tree mortality attributed to spruce beetle, indices of disturbance severity for each mortality agent (Fig. 5). Classification trees indicated that LandTrendr was more likely to detect fire occurrence when RdNBR exceeded 514 (Fig. 5a), and only 52.6% of the total area within fire perimeters exceeded this threshold. Similarly, LandTrendr detection of spruce beetle was most likely when grey-stage tree mortality exceeded 35% in a 30-m cell (Fig. 5b), and this threshold was exceeded in 45.2% of spruce-dominated stands within fire perimeters. Accuracies from cross-validation of classification trees were 79.3% for fire detection and 61.9% for spruce beetle detection, both higher than the no information rate (Appendix D).

4. Discussion

This study builds upon existing literature describing the effectiveness of LTS algorithms for disturbance detection (e.g., Cohen et al., 2017; Schleeweis et al., 2020; Thomas et al., 2011) by comparing LTS detection in a landscape influenced by multiple disturbances with extensive field data and alternative methods of disturbance mapping. We note three key findings: 1) successful detection of the occurrence and timing of tree mortality was strongly related to disturbance type and severity, 2) LandTrendr predicted a substantially lower area affected by disturbance than did other mapping methods, particularly when disturbances occurred at low severity, and 3) factors related to prior disturbance and disturbance overlap had little influence on detection by LandTrendr.

Ecological disturbances operate across a range of spatiotemporal scales and have a broad array of impacts on forest ecosystems. Fire can occur in only moments, but insect outbreaks may take several years to unfold within a stand (Hart et al., 2017; Meddens and Hicke, 2014). Similarly, forest disturbances range from localized removals of plant biomass to stand-replacing events that span broad areas (Agee, 1996; Turner, 2010). Because disturbances encompass a diversity of ecological processes, it is clear that there are certain conditions under which disturbance detection is a challenging task for LTS algorithms. Our finding that LandTrendr was more likely to correctly detect wildfire than spruce beetle outbreaks in field plots, and that detectability of both disturbance types increased with severity, has potentially broad implications for the use of LTS algorithms in disturbance mapping. Gradual, low-severity disturbances (e.g., background tree mortality, non-stand replacing disturbance) are pervasive throughout many forest systems (Cohen et al., 2016; Das et al., 2016; Hermosilla et al., 2019; Shang et al., 2020), but these events can be difficult to separate from other sources of

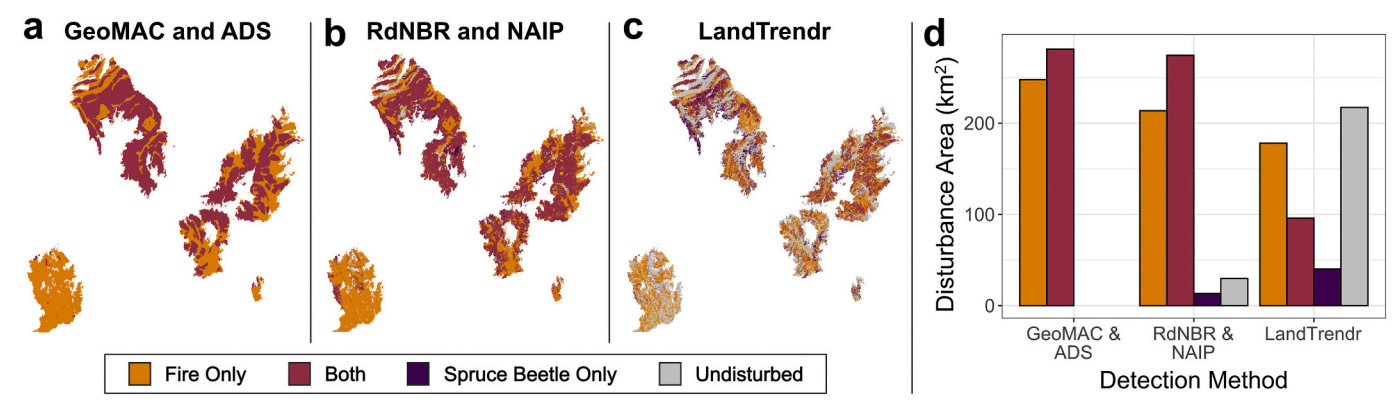


Fig. 4. A comparison of three methods used for mapping fire- and spruce beetle-affected area in the San Juan Mountains, Colorado, USA. In (a), mapped fire perimeters from Wildland Fire Support Geospatial Multi-Agency Coordination (GeoMAC; GeoMAC, 2020) are overlaid with US Forest Service Aerial Detection Survey (ADS; USFS ADS, 2020) polygons that identify tree mortality attributed to spruce beetle. In (b), we used the Relative differenced Normalized Burn Ratio (RdNBR; Miller and Thode, 2007) to identify burned areas within each fire perimeter, and a 3-m thematic map of tree mortality (Hart and Veblen, 2015) derived from National Agriculture Imagery Program (NAIP; USFS NAIP, 2020) imagery to identify pre-fire spruce beetle activity. In (c), we used LandTrendr (Landsat-based Detection of Trends in Disturbance and Recovery; Kennedy et al., 2010) to detect fire and spruce beetle disturbances in the study area. Panel (d) compares the mapped area with only fire (orange), fire and spruce beetle overlap (red), only spruce beetle (purple), and undisturbed area (grey) using each mapping method. (For interpretation of the references to colour in this figure legend, the reader is referred to the web version of this article.)

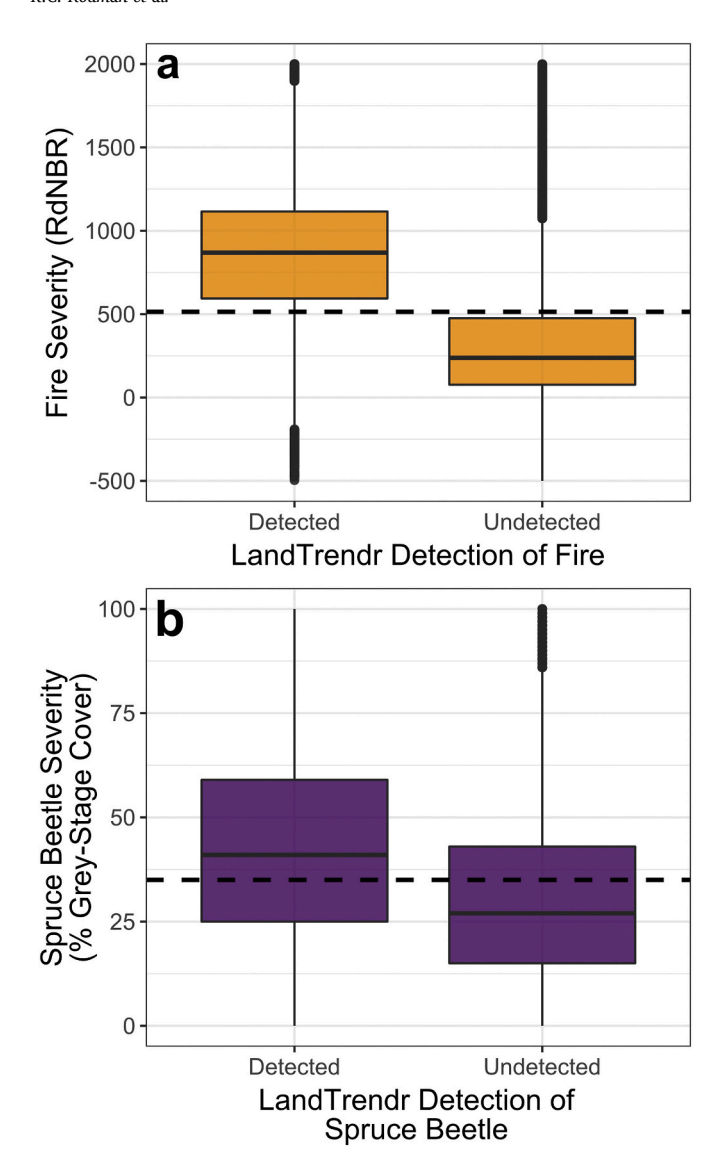


Fig. 5. A comparison of mapped disturbance severity in cells with and without detection of disturbance using LandTrendr (Landsat-based Detection of Trends in Disturbance and Recovery; Kennedy et al., 2010). Fire severity is represented using the Relative differenced Normalized Burn Ratio (RdNBR; Miller and Thode, 2007) calculated from annual pre- and post-fire imagery. Spruce beetle severity is the percent cover of grey-stage tree mortality within each 30-m pixel (Hart and Veblen, 2015). Dashed lines represent a binary split in the data (based on a classification tree model) at which LandTrendr is most likely to detect a disturbance event.

spectral variation in LTS such as unresolved geometric and atmospheric effects and variation in vegetation phenology (Kennedy et al., 2010; Zhu, 2017). Thus, it is likely that the occurrence and timing of many gradual and low-severity disturbances are incorrectly detected in broad-scale mapping efforts using automated LTS algorithms.

In addition to LTS algorithms, several alternative mapping approaches can be used to identify tree-killing disturbances in forest ecosystems. For bark beetle outbreaks and wildfire, perimeters describing total extent can be used to quickly calculate disturbed area across broad regions (e.g., Bentz et al., 2009; Hanes et al., 2019). Another common approach is the use of two-date change indices or image classification with input from analysts to refine the location and timing of occurrence (e.g., Hart and Veblen, 2015; Meddens et al., 2013). Our findings indicate that LandTrendr predicted a c. 40% lower area of disturbance than did either of these alternative approaches. Other studies have effectively

reduced mapping error of LTS products through the use of multispectral ensembles, a combination of algorithms or base learners, or the incorporation of additional data from other satellite systems (e.g., Sentinel-1 and Sentinel-2 missions) (Cohen et al., 2020; Healey et al., 2018; Senf and Seidl, 2020; Shimizu et al., 2019). The inclusion of several spectral bands and indices, particularly those that target the shortwave-infrared portion of the electromagnetic spectrum (e.g., TM-equivalent bands 5 and 7, the Normalized Difference Moisture Index) will improve mapping accuracy in future studies using LTS algorithms (Cohen et al., 2018). Supervised image classification and ancillary datasets such as ADS and the Forest Inventory and Analysis (FIA) monitoring network can also be used to constrain or adjust LTS outputs (Meigs et al., 2015; Schroeder et al., 2014). To refine disturbance detection, hybrid approaches are being developed that include the initial processing steps of LTS algorithms (e.g., developing cloud- and shadow-free annual image composites), but use alternative data sources (Meigs and Krawchuk, 2018), or algorithms tailored to specific disturbance types (Bright et al., 2020). Automated LTS algorithms have clear advantages over alternative approaches when applied across broad areas without detailed knowledge of the type, location, and timing of disturbance events. Still, whenever possible, incorporating additional data may substantially improve the results of LTS-based disturbance detection.

Overlapping forest disturbances are of broad importance because of the potential for linked interactions that influence disturbance properties (e.g. extent or severity; Simard et al., 2011) or compounded interactions that may limit ecosystem recovery (Paine et al., 1998). Remotely sensed data, including LTS products, play an important role in understanding linked and compounded disturbance interactions (Hermosilla et al., 2019; Meigs et al., 2016). We expected that LTS detection might be limited in areas of disturbance overlap because prior disturbance would alter forest structure and change the spectral characteristics of subsequent disturbance. Additionally, we expected that two disturbance events occurring in short succession might be combined during temporal segmentation. Instead, we found that LandTrendr detection was unrelated to the time between disturbances or the severity of prior disturbances. A warming climate is expected to become increasingly suitable for the occurrence and spread of drought-mediated disturbances such as wildfire and bark beetle outbreaks (Abatzoglou et al., 2019; Bentz et al., 2010), leading to increases in the total area of disturbance overlap. Similarly, with the planned launch of Landsat-9 and the increasing length of the Landsat record (Wulder et al., 2019), disturbance overlap in LTS will be an increasingly common issue. Our findings support the use of LTS-based approaches for the detection and monitoring of overlapping disturbances. Still, we tested only one combination of disturbance events (bark beetle followed by wildfire) and additional work is needed to determine if LTS algorithms are similarly effective with other sequences and types of disturbance (e.g., wildfire followed by insects, insect outbreaks followed by salvage logging), and alternative forest types.

In the present study, we primarily focused on errors of omission, or the failure to detect disturbances in areas of known occurrence. Omission and commission error are inversely related (Cohen et al., 2017; Congalton, 1991) and LTS algorithms that are capable of detecting disturbances associated with minor spectral changes will inherently have a greater number of false detections. Thus, designing increasingly sensitive LTS algorithms is not an effective means of reducing mapping error unless outputs are paired with ancillary data that can limit false positives. We specifically assessed vertex agreement, the agreement of LTS-detected occurrence and timing of disturbance with observed or analyst-interpreted timing, but many additional accuracy measures can also be used to assess the effectiveness of LTS algorithms (Cohen et al., 2010). However, vertex agreement is a particularly useful measure of accuracy in LTS detection because it assesses one of the key advantages of LTS over two-date approaches, the accurate representation of the timing and rate of events (Kennedy et al., 2014).

LTS algorithms are commonly used for forest ecosystem monitoring,

and their use is likely to increase in the future (Banskota et al., 2014; Zhu, 2017). An assessment of the causes of mapping error and uncertainty in LTS products aids in methodological refinement, which in turn improves the effectiveness of monitoring efforts that have broad implications for science, policy, and society. Herein, we note that a commonly used LTS algorithm more easily detects severe and abrupt disturbances than gradual and low-severity disturbances. Users of LTS algorithms should be aware of potential biases in derived products, including omission of low-severity disturbances, and how these biases may influence monitoring efforts. Yet we also noted that LTS detection was robust to disturbance overlap, an important finding that supports the use of LTS algorithms in areas with a complex history of natural and anthropogenic disturbances. With the increasing length of the Landsat record and the increasing availability of additional data sources (e.g., Sentinel-2, MODIS), automated algorithms using image time series will continue to play a crucial role in understanding and addressing human impacts and ecosystem changes across Earth's surface.

Data availability statement

All data and statistical analyses associated with this paper are available through the Dryad Digital Repository: https://doi.org/10.5061/dryad.dv41ns1ws (Rodman et al., 2020).

Declaration of Competing Interest

The authors declare that they have no known competing financial interests or personal relationships that could have appeared to influence the work reported in this paper.

Acknowledgements

This research was funded by National Science Foundation awards 1262687 and 1853520 and National Aeronautics and Space Administration award NNX16AH58G. Support for this research was also provided by the University of Wisconsin–Madison, Office of the Vice Chancellor for Research and Graduate Education with funding from the Wisconsin Alumni Research Foundation. The authors would like to thank Cornelius Senf and an anonymous reviewer for helpful comments that improved a previous version of this manuscript.

Appendix A. Supplementary data

Supplementary data to this article can be found online at https://doi. org/10.1016/j.rse.2020.112244.

References

- Abatzoglou, J.T., Williams, A.P., Barbero, R., 2019. Global emergence of anthropogenic climate change in fire weather indices. Geophys. Res. Lett. 46, 326–336.
- Agee, J.K., 1996. Fire Ecology of Pacific Northwest Forests, 2nd ed. Island Press, Washington D. C.
- Andrus, R.A., Veblen, T.T., Harvey, B.J., Hart, S.J., 2016. Fire severity unaffected by spruce beetle outbreak in spruce-fir forests in southwestern Colorado. Ecol. Appl. 26, 700–711.
- Andrus, R.A., Hart, S.J., Veblen, T.T., 2020. Forest recovery following synchronous outbreaks of spruce and western balsam bark beetle is slowed by ungulate browsing. Ecology 101, 1–13.
- Awty-Carroll, K., Bunting, P., Hardy, A., Bell, G., 2019. An evaluation and comparison of four dense time series change detection methods using simulated data. Remote Sens. 11, 2779.
- Baker, W.L., Veblen, T.T., 1990. Spruce beetles and fires in the nineteenth-century subalpine forests of western Colorado. USA. Arct. Alp. Res. 22, 65–80.
- Banskota, A., Kayastha, N., Falkowski, M.J., Wulder, M.A., Froese, R.E., White, J.C., 2014. Forest monitoring using Landsat time series data: a review. Can. J. Remote. Sens. 40, 362–384.
- Bartón, K., 2018. MuMIn: Multi-model inference. R package. URL. https://cran.r-project.org/web/packages/MuMIn/index.html.
- Bentz, B.J., Logan, J., MacMahon, J., Allen, C.D., Ayres, M., Berg, E., Carroll, A.L., Hansen, M.C., Hicke, J.A., Joyce, L., Macfarlane, W., Munson, S., Negrón, J.F., Paine, T., Powell, J., Raffa, K.F., Régnière, J., Reid, M.S., Romme, W.H., Seybold, S.

- J., Six, D.L., Tomback, D., Vandygriff, J., Veblen, T.T., White, M., Witcosky, J., Wood, D., 2009. Bark Beetle Outbreaks in Western North America: Causes and Consequences, in: Bark Beetle Symposium. University of Utah Press, Snowbird, UT.
- Bentz, B.J., Régnière, J., Fettig, C.J., Hansen, E.M., Hayes, J.L., Hicke, J.A., Kelsey, R.G., Negrón, J.F., Seybold, S.J., 2010. Climate change and bark beetles of the western United States and Canada: direct and indirect effects. BioScience 60, 602–613.
- Bjornstad, O.N., 2019. ncf: Spatial Covariance Functions. R package. URL. https://cran.r-project.org/web/packages/ncf/index.html.
- Bolker, B.M., Brooks, M.E., Clark, C.J., Geange, S.W., Poulsen, J.R., Stevens, M.H.H., White, J.-S.S., 2009. Generalized linear mixed models: a practical guide for ecology and evolution. Trends Ecol. Evol. 24, 127–135.
- Bonan, G.B., 2008. Forests and climate change: forcings, feedbacks, and the climate benefits of forests. Science 320, 1444–1449.
- Breiman, L., Friedman, J., Stone, C.J., Olshen, R.A., 1984. Classification and Regression Trees. Chapman and Hall/CRC, Boca Raton, FL.
- Bright, B.C., Hudak, A.T., Meddens, A.J.H., Egan, J.M., Jorgensen, C.L., 2020. Mapping multiple insect outbreaks across large regions annually using Landsat time series data. Remote Sens. 12, 1–21.
- Brooks, M.E., Kristensen, K., van Benthem, K.J., Magnusson, A., Berg, C.W., Nielsen, A., Skaug, H.J., Maechler, M., Bolker, B.M., 2017. glmmTMB balances speed and flexibility among packages for zero-inflated generalized linear mixed modeling. R J. 9, 378–400.
- Buechling, A., Baker, W.L., 2004. A fire history from tree rings in a high-elevation forest of Rocky Mountain National Park. Can. J. For. Res. 34, 1259–1273.
- Carlson, A.R., Sibold, J.S., Assal, T.J., Negrón, J.F., 2017. Evidence of compounded disturbance effects on vegetation recovery following high-severity wildfire and spruce beetle outbreak. PLoS One 12, 1–24.
- Cohen, W.B., Yang, Z., Kennedy, R., 2010. Detecting trends in forest disturbance and recovery using yearly Landsat time series: 2. TimeSync - tools for calibration and validation. Remote Sens. Environ. 114, 2911–2924.
- Cohen, W.B., Yang, Z., Stehman, S.V., Schroeder, T.A., Bell, D.M., Masek, J.G., Huang, C., Meigs, G.W., 2016. Forest disturbance across the conterminous United States from 1985-2012: the emerging dominance of forest decline. For. Ecol. Manag. 360, 242–252.
- Cohen, W.B., Healey, S.P., Yang, Z., Stehman, S.V., Brewer, C.K., Brooks, E.B., Gorelick, N., Huang, C., Hughes, M.J., Kennedy, R.E., Loveland, T.R., Moisen, G.G., Schroeder, T.A., Vogelmann, J.E., Woodcock, C.E., Yang, L., Zhu, Z., 2017. How similar are forest disturbance maps derived from different Landsat time series aleorithms? Forests 8. 1–19.
- Cohen, W.B., Yang, Z., Healey, S.P., Kennedy, R.E., Gorelick, N., 2018. A LandTrendr multispectral ensemble for forest disturbance detection. Remote Sens. Environ. 205, 131–140.
- Cohen, W.B., Healey, S.P., Yang, Z., Zhu, Z., Gorelick, N., 2020. Diversity of algorithm and spectral band inputs improves Landsat monitoring of forest disturbance. Remote Sens. 12, 1–15.
- Congalton, R.G., 1991. A review of assessing the accuracy of classifications of remotely sensed data. Remote Sens. Environ. 37, 35–46.
- Das, A.J., Stephenson, N.L., Davis, K.P., 2016. Why do trees die? Characterizing the drivers of background tree mortality. Ecology 97, 2616–2627.
- Eidenshink, J., Schwind, B., Brewer, K., Zhu, Z., Quayle, B., Howard, S., Falls, S., Falls, S., 2007. A project for monitoring trends in burn severity. Fire Ecol. 3, 3–21.
- Flood, N., 2013. Seasonal composite Landsat TM/ETM+ images using the medoid (a multi-dimensional median). Remote Sens. 5, 6481–6500.
- Foga, S., Scaramuzza, P.L., Guo, S., Zhu, Z., Dilley, R.D., Beckmann, T., Schmidt, G.L., Dwyer, J.L., Joseph Hughes, M., Laue, B., 2017. Cloud detection algorithm comparison and validation for operational Landsat data products. Remote Sens. Environ. 194, 379–390.
- Foster, A.C., Walter, J.A., Shugart, H.H., Sibold, J., Negron, J., 2017. Spectral evidence of early-stage spruce beetle infestation in Engelmann spruce. For. Ecol. Manag. 384, 347–357.
- Gelman, A., 2008. Scaling regression inputs by dividing by two standard deviations. Stat. Med. 27, 2865–2873.
- Geospatial Multi-agency Coordinating Group (GeoMAC) [WWW Document], 2020. Hist. fire data. URL https://rmgsc.cr.usgs.gov/outgoing/GeoMAC/ (accessed 2.25.20).
- Gorelick, N., Hancher, M., Dixon, M., Ilyushchenko, S., Thau, D., Moore, R., 2017. Google Earth Engine: planetary-scale geospatial analysis for everyone. Remote Sens. Environ. 202, 18–27.
- Grime, J.P., 1979. Plant Strategies, Vegetation Processes, and Ecosystem Properties. John Wiley & Sons, Chichester, England.
- Hanes, C.C., Wang, X., Jain, P., Parisien, M.A., Little, J.M., Flannigan, M.D., 2019. Fire-regime changes in Canada over the last half century. Can. J. For. Res. 49, 256–269.
- Hart, S.J., Veblen, T.T., 2015. Detection of spruce beetle-induced tree mortality using high- and medium-resolution remotely sensed imagery. Remote Sens. Environ. 168, 134–145.
- Hart, S.J., Veblen, T.T., Kulakowski, D., 2014. Do tree and stand-level attributes determine susceptibility of spruce-fir forests to spruce beetle outbreaks in the early 21st century? For. Ecol. Manag. 318, 44–53.
- Hart, S.J., Veblen, T.T., Schneider, D., Molotch, N.P., 2017. Summer and winter drought drive the initiation and spread of spruce beetle outbreak. Ecology 98, 2698–2707.
- Hartig, F., 2018. Package 'DHARMa': Residual Diagnostics for Hierarchical (Multi-Level/Mixed) Regression Models. URL. https://cran.r-roject.org/web/packages/DHARMa/vignettes/DHARMa.html.
- Harvey, B.J., Donato, D.C., Romme, W.H., Turner, M.G., 2013. Influence of recent bark beetle outbreak on fire severity and postfire tree regeneration in montane Douglas-fir forests. Ecology 94, 2475–2486.

- Harvey, B.J., Andrus, R.A., Anderson, S.C., 2019. Incorporating biophysical gradients and uncertainty into burn severity maps in a temperate fire-prone forested region. Ecosphere 10, e02600.
- Healey, S.P., Cohen, W.B., Yang, Z., Kenneth Brewer, C., Brooks, E.B., Gorelick, N., Hernandez, A.J., Huang, C., Joseph Hughes, M., Kennedy, R.E., Loveland, T.R., Moisen, G.G., Schroeder, T.A., Stehman, S.V., Vogelmann, J.E., Woodcock, C.E., Yang, L., Zhu, Z., 2018. Mapping forest change using stacked generalization: an ensemble approach. Remote Sens. Environ. 204, 717–728.
- Hermosilla, T., Wulder, M.A., White, J.C., Coops, N.C., Hobart, G.W., Campbell, L.B., 2016. Mass data processing of time series Landsat imagery: pixels to data products for forest monitoring. Int. J. Digit. Earth 9, 1035–1054.
- Hermosilla, T., Wulder, M.A., White, J.C., Coops, N.C., 2019. Prevalence of multiple forest disturbances and impact on vegetation regrowth from interannual Landsat time series (1985–2015). Remote Sens. Environ. 233, 111403.
- Hicke, J.A., Meddens, A.J.H., Kolden, C.A., 2016. Recent tree mortality in the western United States from bark beetles and forest fires. For. Sci. 62, 141–153.
- Homer, C., Dewitz, J., Jin, S., Xian, G., Costello, C., Danielson, P., Gass, L., Funk, M., Wickham, J., Stehman, S., Auch, R., Riitters, K., 2020. Conterminous United States land cover change patterns 2001–2016 from the 2016 National Land Cover Database. ISPRS J. Photogramm. Remote Sens. 162, 184–199.
- Hothorn, T., Hornik, K., Zeileis, A., 2014. Party: A Laboratory for Recursive Part(y) Tioning. URL. https://cran.r-project.org/web/packages/party/vignettes/party.pdf.
- Huang, C., Goward, S.N., Masek, J.G., Thomas, N., Zhu, Z., Vogelmann, J.E., 2010. An automated approach for reconstructing recent forest disturbance history using dense Landsat time series stacks. Remote Sens. Environ. 114, 183–198.
- Hughes, M.J., Douglas Kaylor, S., Hayes, D.J., 2017. Patch-based forest change detection from Landsat time series. Forests 8, 1–22.
- Jenkins, M.J., Hebertson, E.G., Munson, A.S., 2014. Spruce beetle biology, ecology and management in the Rocky Mountains: an addendum to spruce beetle in the Rockies. Forests 5, 21–71.
- Kennedy, R.E., Yang, Z., Cohen, W.B., 2010. Detecting trends in forest disturbance and recovery using yearly Landsat time series: 1. LandTrendr - temporal segmentation algorithms. Remote Sens. Environ. 114, 2897–2910.
- Kennedy, R.E., Yang, Z., Cohen, W.B., Pfaff, E., Braaten, J., Nelson, P., 2012. Spatial and temporal patterns of forest disturbance and regrowth within the area of the Northwest Forest Plan. Remote Sens. Environ. 122, 117–133.
- Kennedy, R.E., Andréfouët, S., Cohen, W.B., Gómez, C., Griffiths, P., Hais, M., Healey, S. P., Helmer, E.H., Hostert, P., Lyons, M.B., Meigs, G.W., Pflugmacher, D., Phinn, S.R., Powell, S.L., Scarth, P., Sen, S., Schroeder, T.A., Schneider, A., Sonnenschein, R., Vogelmann, J.E., Wulder, M.A., Zhu, Z., 2014. Bringing an ecological view of change to Landsat-based remote sensing. Front. Ecol. Environ. 12, 339–346.
- Kennedy, R.E., Yang, Z., Gorelick, N., Braaten, J., Cavalcante, L., Cohen, W.B., Healey, S., 2018. Implementation of the LandTrendr algorithm on Google Earth Engine. Remote Sens. 10, 691.
- Key, C.H., Benson, N.C., 2006. Landscape assessment (LA): sampling and analysis methods. In: Lutes, D.C. (Ed.), FIREMON: fire Effects Monitoring and Inventory System. RMRS-GTR-164-CD. Rocky Mountain Research Station, USDA Forest Service, Fort Collins, CO, pp. LA1–LA51.
- Kolden, C.A., Lutz, J.A., Key, C.H., Kane, J.T., van Wagtendonk, J.W., 2012. Mapped versus actual burned area within wildfire perimeters: characterizing the unburned. For. Ecol. Manag. 286, 38–47.
- Kolden, C.A., Smith, A.M.S., Abatzoglou, J.T., 2015. Limitations and utilisation of monitoring trends in burn severity products for assessing wildfire severity in the USA. Int. J. Wildland Fire 24, 1023–1028.
- Lalande, B.M., Hughes, K., Jacobi, W.R., Tinkham, W.T., Reich, R., Stewart, J.E., 2020. Subalpine fir mortality in Colorado is associated with stand density, warming climates and interactions among fungal diseases and the western balsam bark beetle. For. Ecol. Manag. 466, 118133.
- McDowell, N.G., Allen, C.D., Anderson-Teixeira, K., Aukema, B.H., Bond-Lamberty, B., Chini, L., Clark, J.S., Dietze, M., Grossiord, C., Hanbury-brown, A., Hurtt, G.C., Jackson, R.B., Johnson, D.J., Kueppers, L., Lichstein, J.W., Ogle, K., Poulter, B., Pugh, T.A.M., Seidl, R., Turner, M.G., Uriarte, M., Walker, A.P., Xu, C., 2020. Pervasive shifts in forest dynamics in a changing world. Science 368 eaaz9463.
- Meddens, A.J.H., Hicke, J.A., 2014. Spatial and temporal patterns of Landsat-based detection of tree mortality caused by a mountain pine beetle outbreak in Colorado. USA. For. Ecol. Manage. 322, 78–88.
- Meddens, A.J.H., Hicke, J.A., Vierling, L.A., Hudak, A.T., 2013. Evaluating methods to detect bark beetle-caused tree mortality using single-date and multi-date Landsat imagery. Remote Sens. Environ. 132, 49–58.
- Meddens, A.J.H., Kolden, C.A., Lutz, J.A., 2016. Detecting unburned areas within wildfire perimeters using Landsat and ancillary data across the northwestern United States. Remote Sens. Environ. 186, 275–285.
- Meigs, G.W., Krawchuk, M.A., 2018. Composition and structure of forest fire refugia: what are the ecosystem legacies across burned landscapes? Forests 9, 243.
- Meigs, G.W., Kennedy, R.E., Gray, A.N., Gregory, M.J., 2015. Spatiotemporal dynamics of recent mountain pine beetle and western spruce budworm outbreaks across the Pacific Northwest Region. USA. For. Ecol. Manage. 339, 71–86.
- Meigs, G.W., Zald, H.S.J., Campbell, J.L., Keeton, W.S., Kennedy, R.E., 2016. Do insect outbreaks reduce the severity of subsequent forest fires? Environ. Res. Lett. 11, 1–10.
- Meigs, G.W., Dunn, C.J., Parks, S.A., Krawchuk, M.A., 2020. Influence of topography and fuels on fire refugia probability under varying fire weather in forests of the US Pacific Northwest. Can. J. For. Res. 50, 636–647.
- Miller, J.D., Thode, A.E., 2007. Quantifying burn severity in a heterogeneous landscape with a relative version of the Delta Normalized Burn Ratio (dNBR). Remote Sens. Environ. 109, 66–80.

- Miller, J.D., Knapp, E.E., Key, C.H., Skinner, C.N., Isbell, C.J., Creasy, R.M., Sherlock, J. W., 2009. Calibration and validation of the relative differenced normalized burn ratio (RdNBR) to three measures of fire severity in the Sierra Nevada and Klamath Mountains, California. USA. Remote Sens. Environ. 113, 645–656.
- National Agriculture Imagery Progam, USDA Forest Service [WWW dDocument], 2020. URL http://www.fsa.usda.gov/programs-and-services/aerial-photography/imagery-programs/naip-imagery/ (accessed 2.8.20).
- Paine, R.T., Tegner, M.J., Johnson, E.A., 1998. Compunded perturbations yield ecological surprises. Ecosystems 1, 535–545.
- Parks, S.A., Miller, C., Nelson, C.R., Holden, Z.A., 2014. Previous fires moderate burn severity of subsequent wildland fires in two large western US wilderness areas. Ecosystems 17, 29–42.
- Parks, S.A., Holsinger, L.M., Voss, M.A., Loehman, R.A., Robinson, N.P., 2018. Mean composite fire severity metrics computed with Google Earth Engine offer improved accuracy and expanded mapping potential. Remote Sens. 10, 1–15.
- Pengra, B., Gallant, A.L., Zhu, Z., Dahal, D., 2016. Evaluation of the initial thematic output from a continuous change-detection algorithm for use in automated operational land-change mapping by the U.S. Geological Survey. Remote Sens. 8, 1–33
- PRISM Climate Group, Oregon State University [WWW Document], 2020. URL http://prism.oregonstate.edu (accessed 2.25.20).
- Raffa, K.F., Aukema, B.H., Bentz, B.J., Carroll, A.L., Hicke, J.A., Turner, M.G., Romme, W.H., 2008. Cross-scale drivers of natural disturbances prone to anthropogenic amplification: the dynamics of bark beetle eruptions. BioScience 58, 501.
- R-Core-Team, 2018. R: A Language and Environment for Statistical Computing. URL. https://www.r-project.org/.
- Region 2 Aerial Detection Survey [WWW Document], 2020. URL https://www.fs.usda.gov/detail/r2/forest-grasslandhealth/?cid=fsbdev3_041629 (accessed 3.1.20).
- Rodman, K.C., Andrus, R.A., Veblen, T.T., Hart, S.J., 2020. Data from: disturbance detection in Landsat time series is influenced by tree mortality agent and severity, not by prior disturbance. Dryad. https://doi.org/10.5061/dryad.dv41ns1ws.
- Rollins, M.G., 2009. LANDFIRE: a nationally consistent vegetation, wildland fire, and fuel assessment. Int. J. Wildland Fire 18, 235–249.
- Romme, W.H., Floyd, M.L., Hanna, D., Bartlett, E.J., Crist, M., Green, D., Grissino-Mayer, H.D., Lindsey, J.P., McGarigal, K., Redders, J.S., 2009. Historical Range of Variability and Current Landscape Condition Analysis: South Central Highlands Section, Southwestern Colorado and Northwestern New Mexico. Fort Collins, CO., Colorado Forest Restoration Institute.
- Roy, D.P., Kovalskyy, V., Zhang, H.K., Vermote, E.F., Yan, L., Kumar, S.S., Egorov, A., 2016. Characterization of Landsat-7 to Landsat-8 reflective wavelength and normalized difference vegetation index continuity. Remote Sens. Environ. 185, 57–70.
- Savage, S.L., Lawrence, R.L., Squires, J.R., 2017. Mapping post-disturbance forest landscape composition with Landsat satellite imagery. For. Ecol. Manag. 399, 9–23.
- Schleeweis, K., Moisen, G., Toney, C., Schroeder, T., Freeman, E., Goward, S., Huang, C., Dungan, J., 2020. US national maps attributing forest change: 1986-2010. Forests 11, 653.
- Schmid, J.M., Frye, R.H., 1977. Spruce beetle in the Rockies. In: GTR RM-49. Rocky Mountain Forest and Range Experiment Station. USDA Forest Service, Fort Collins, CO.
- Schroeder, T.A., Wulder, M.A., Healey, S.P., Moisen, G.G., 2011. Mapping wildfire and clearcut harvest disturbances in boreal forests with Landsat time series data. Remote Sens. Environ. 115, 1421–1433.
- Schroeder, T.A., Healey, S.P., Moisen, G.G., Frescino, T.S., Cohen, W.B., Huang, C., Kennedy, R.E., Yang, Z., 2014. Improving estimates of forest disturbance by combining observations from Landsat time series with U.S. Forest Service Forest Inventory and Analysis data. Remote Sens. Environ. 154, 61–73.
- Senf, C., Seidl, R., 2020. Mapping the forest disturbance regimes of Europe. Nat. Sustain. https://doi.org/10.1038/s41893-020-00609-y.
 Senf, C., Pflugmacher, D., Wulder, M.A., Hostert, P., 2015. Characterizing spectral-
- Senf, C., Pflugmacher, D., Wulder, M.A., Hostert, P., 2015. Characterizing spectraltemporal patterns of defoliator and bark beetle disturbances using Landsat time series. Remote Sens. Environ. 170, 166–177.
- Senf, C., Seidl, R., Hostert, P., 2017. Remote sensing of forest insect disturbances: current state and future directions. Int. J. Appl. Earth Obs. Geoinf. 60, 49–60.
- Shang, C., Coops, N.C., Wulder, M.A., White, J.C., Hermosilla, T., 2020. Update and spatial extension of strategic forest inventories using time series remote sensing and modeling. Int. J. Appl. Earth Obs. Geoinf. 84, 101956.
- Shimizu, K., Ota, T., Mizoue, N., 2019. Detecting forest changes using dense Landsat 8 and Sentinel-1 time series data in tropical seasonal forests. Remote Sens. 11, 1–22.
- Sibold, J.S., Veblen, T.T., 2006. Relationships of subalpine forest fires in the Colorado Front Range to interannual and multi-decadal scale climate variations. J. Biogeogr. 33, 833–842.
- Simard, M., Romme, W.H., Griffin, J.M., Turner, M.G., 2011. Do mountain pine beetle outbreaks change the probability of active crown fire in lodgepole pine forests? Ecol. Monogr. 81, 3–24.
- Temperli, C., Hart, S.J., Veblen, T.T., Kulakowski, D., Hicks, J.J., Andrus, R., 2014. Are density reduction treatments effective at managing for resistance or resilience to spruce beetle disturbance in the southern Rocky Mountains? For. Ecol. Manag. 334, 53–63.
- Thom, D., Seidl, R., 2016. Natural disturbance impacts on ecosystem services and biodiversity in temperate and boreal forests. Biol. Rev. Camb. Philos. Soc. 91, 760–781.
- Thomas, N.E., Huang, C., Goward, S.N., Powell, S., Rishmawi, K., Schleeweis, K., Hinds, A., 2011. Validation of North American forest disturbance dynamics derived from Landsat time series stacks. Remote Sens. Environ. 115, 19–32.

- Trumbore, S., Brando, P., Hartmann, H., 2015. Forest health and global change. Science 349, 814–818.
- Turner, M.G., 2010. Disturbance and landscape dynamics in a changing world. Ecology 91, 2833–2849.
- USDA Forest Service Geodata downloadable national datasets [WWW Document], 2020. URL https://data.fs.usda.gov/geodata/edw/datasets.php (accessed 2.20.20).
- White, J.C., Wulder, M.A., Hermosilla, T., Coops, N.C., Hobart, G.W., 2017. A nationwide annual characterization of 25 years of forest disturbance and recovery for Canada using Landsat time series. Remote Sens. Environ. 194, 303–321.
- Wilson, B.T., Lister, A.J., Riemann, R.I., Griffith, D.M., 2013. Live Tree Species Basal Area of the Contiguous United States (2000-2009). St. Paul, MN, USA. URL. https://www.fs.usda.gov/rds/archive/catalog/RDS-2013-0013.
- Wulder, M.A., Loveland, T.R., Roy, D.P., Crawford, C.J., Masek, J.G., Woodcock, C.E., Allen, R.G., Anderson, M.C., Belward, A.S., Cohen, W.B., Dwyer, J., Erb, A., Gao, F.,
- Griffiths, P., Helder, D., Hermosilla, T., Hipple, J.D., Hostert, P., Hughes, M.J., Huntington, J., Johnson, D.M., Kennedy, R., Kilic, A., Li, Z., Lymburner, L., McCorkel, J., Pahlevan, N., Scambos, T.A., Schaaf, C., Schott, J.R., Sheng, Y., Storey, J., Vermote, E., Vogelmann, J., White, J.C., Wynne, R.H., Zhu, Z., 2019. Current status of Landsat program, science, and applications. Remote Sens. Environ. 225, 127–147.
- Zhu, Z., 2017. Change detection using Landsat time series: a review of frequencies, preprocessing, algorithms, and applications. ISPRS J. Photogramm. Remote Sens. 130, 370–384.
- Zhu, Z., Zhang, J., Yang, Z., Aljaddani, A.H., Cohen, W.B., Qiu, S., Zhou, C., 2020. Continuous monitoring of land disturbance based on Landsat time series. Remote Sens. Environ. 238, 111116.
- Zuur, A.F., Ieno, E.N., Walker, N.J., Saveliev, A.A., Smith, G.M., 2009. Mixed Effects Models and Extensions in Ecology and R. Springer, New York.